Molecular Biology of the Cell
Vol. 21, 979–988, March 15, 2010

Poleward Transport of TPX2 in the Mammalian Mitotic Spindle Requires Dynein, Eg5, and Microtubule Flux

Nan Ma,* U. S. Tulu,† Nick P. Ferenz,* Carey Fagerstrom,* Andrew Wilde,‡ and Patricia Wadsworth*

*University of Massachusetts, Amherst, MA 01003; †Duke University, Durham NC 27708; and ‡University of Toronto, Toronto, Ontario M5S 1A8, Canada

Submitted July 24, 2009; Revised December 29, 2009; Accepted January 15, 2010
Monitoring Editor: Yixian Zheng

TPX2 is a Ran-regulated spindle assembly factor that is required for kinetochore fiber formation and activation of the mitotic kinase Aurora A. TPX2 is enriched near spindle poles and is required near kinetochores, suggesting that it undergoes dynamic relocalization throughout mitosis. Using photoactivation, we measured the movement of PA-GFP-TPX2 in the mitotic spindle. TPX2 moves poleward in the half-spindle and is static in the interzone and near spindle poles. Poleward transport of TPX2 is sensitive to inhibition of dynein or Eg5 and to suppression of microtubule flux with nocodazole or antibodies to Kif2a. Poleward transport requires the C terminus of TPX2, a domain that interacts with Eg5. Overexpression of TPX2 lacking this domain induced excessive microtubule formation near kinetochores, defects in spindle assembly and blocked mitotic progression. Our data support a model in which poleward transport of TPX2 down-regulates its microtubule nucleating activity near kinetochores and links microtubules generated at kinetochores to dynein for incorporation into the spindle.

INTRODUCTION

The mitotic spindle self-assembles from microtubules and associated structural and regulatory proteins and is required for chromosome segregation during cell division. Microtubules, the major structural element of the spindle, are dynamically unstable polymers that alternate stochastically between phases of growth and rapid shortening (Mitchison and Kirschner, 1984). During spindle assembly in mammalian cells, dynamic microtubules nucleated at each centrosome search for and capture kinetochores on replicated chromosomes (Kirschner and Mitchison, 1986). In cells lacking centrosomes, microtubules assemble near chromatin/kinetochores, in a Ran-dependent manner, and are subsequently polarity sorted and organized into a bipolar array (Heald *et al*., 1996; Wilde and Zheng, 1999). Recent work has shown that the chromatin-dependent pathway functions in centrosome containing cells as well: spindle formation can proceed after centrosome destruction or elimination and microtubule formation is observed near chromosomes/kinetochores in cells treated and released from nocodazole (Khodjakov *et al*., 2000; Hinchcliffe *et al*., 2001; Tulu *et al*., 2006). In centrosome-containing cells, microtubules formed near chromatin interact with centrosomal microtubules for incorporation into the spindle (Khodjakov *et al*., 2003). In addition to dynamic instability, spindle microtubules exhibit an additional dynamic behavior called flux, which is characterized by the slow, poleward movement of the microtubule lattice (Mitchison, 1989). At metaphase, spindle flux, or sliding (Burbank *et al*., 2007), is accompanied by the balanced addition and loss of tubulin subunits from microtubule plus-ends near the spindle equator and minus-ends near spindle poles, respectively (Rogers *et al*., 2005).

Many microtubule-associated proteins and molecular motors regulate the nucleation, turnover, and flux of spindle microtubules, but our understanding of the mechanism(s) by which these factors function is still incomplete. TPX2 is a Ran-regulated microtubule-associated protein (Trieselmann *et al*., 2003) that nucleates, binds, and bundles microtubules in vitro; is required for microtubule formation at kinetochores; and contributes to spindle pole organization (Schatz *et al*., 2003; Brunet *et al*., 2004; Tulu *et al*., 2006). TPX2 localizes to spindle fibers but not polar astral microtubules and is enriched at spindle poles (Garrett *et al*., 2002; Gruss *et al*., 2002). The N terminus of TPX2, which binds and activates Aurora A kinase, is required for microtubule nucleation at chromosomes and to establish spindle length (Bayliss *et al*., 2003; Koffa *et al*., 2006; Bird and Hyman, 2008). A large C-terminal domain is required to localize TPX2 to the spindle, and the extreme C terminus interacts with Eg5 (Brunet *et al*., 2004; Eckerdt *et al*., 2008). In *Xenopus laevis* extracts, TPX2 is part of the hepatoma up-regulated protein (HURP) complex, which is composed of XMAP215, Aurora A, Eg5, TPX2, and HURP and is required for Ran-dependent bipolar spindle formation (Koffa *et al*., 2006).

Localization of the kinesin Xklp2 to spindle poles requires TPX2 and dynein (Wittmann *et al*., 1998). Dynein activity is also required for the poleward transport of the plus-end–directed bipolar kinesin Eg5, which interacts with the p150 subunit of dynactin as well as with TPX2 (Blangy *et al*., 1997; Eckerdt *et al*., 2008; Uteng *et al*., 2008). Based on these observations, we hypothesized that in the half-spindle, TPX2, alone or as part of a larger complex, is transported poleward, leading to its accumulation at microtubule minus-ends. Using photoactivation, we report that TPX2 is transported in the half-spindle and is static on inter-

This article was published online ahead of print in *MBC in Press* (http://www.molbiolcell.org/cgi/doi/10.1091/mbc.E09–07–0601) on January 28, 2010.

Address correspondence to: Patricia Wadsworth (patw@bio.umass.edu).

zonal microtubules. TPX2 transport in the half-spindle is sensitive to inhibition of Eg5 and dynein and to suppression of microtubule flux with nocodazole. The C-terminal 35 amino acids of TPX2, which interact with Eg5, are required for poleward transport.

MATERIALS AND METHODS

All materials for cell culture were obtained from Sigma-Aldrich (St. Louis, MO), with the exception of Opti-MEM, which was obtained from Invitrogen (Carlsbad, CA) and fetal bovine serum, which was obtained from Altanta Biologicals (Norcross, GA). Unless otherwise noted, all other chemicals were obtained from Sigma-Aldrich.

Cell Culture and Immunofluorescence

Parental LLC-Pk1 cells and LLC-Pk1 cells expressing enhanced green fluorescent protein (EGFP)-α-tubulin (referred to here as LLC-Pk1-α) were grown as described previously (Tulu *et al.*, 2003). For immunofluorescence, cells were rinsed twice in warm, calcium- and magnesium-free phosphate-buffered saline ($PBS^{-/-}$), followed by fixation in ice-cold methanol or 3.2% paraformaldehyde, 0.1% glutaraldehyde, and 0.5% Triton in $PBS^{-/-}$. Fixed cells were rinsed in $PBS^{-/-}$ containing 0.02% sodium azide and 0.1% Tween 20. The following primary antibodies were used in these experiments: MCAK, gift from Dr. Claire Walczak (Indiana University, Bloomington, IN); Mad2, a gift from Dr. Alexey Khodjakov (Wadsworth Center, Albany, NY); YL½ (Accurate Chemical, Westbury, NY); Hec1, TPX2, and Kif2a (Novus Biologicals, Littleton, CO); and p150 (BD Biosciences, Franklin Lakes, NJ). Incubations with primary antibodies were performed for 1 h at 37°C, using the manufactur-

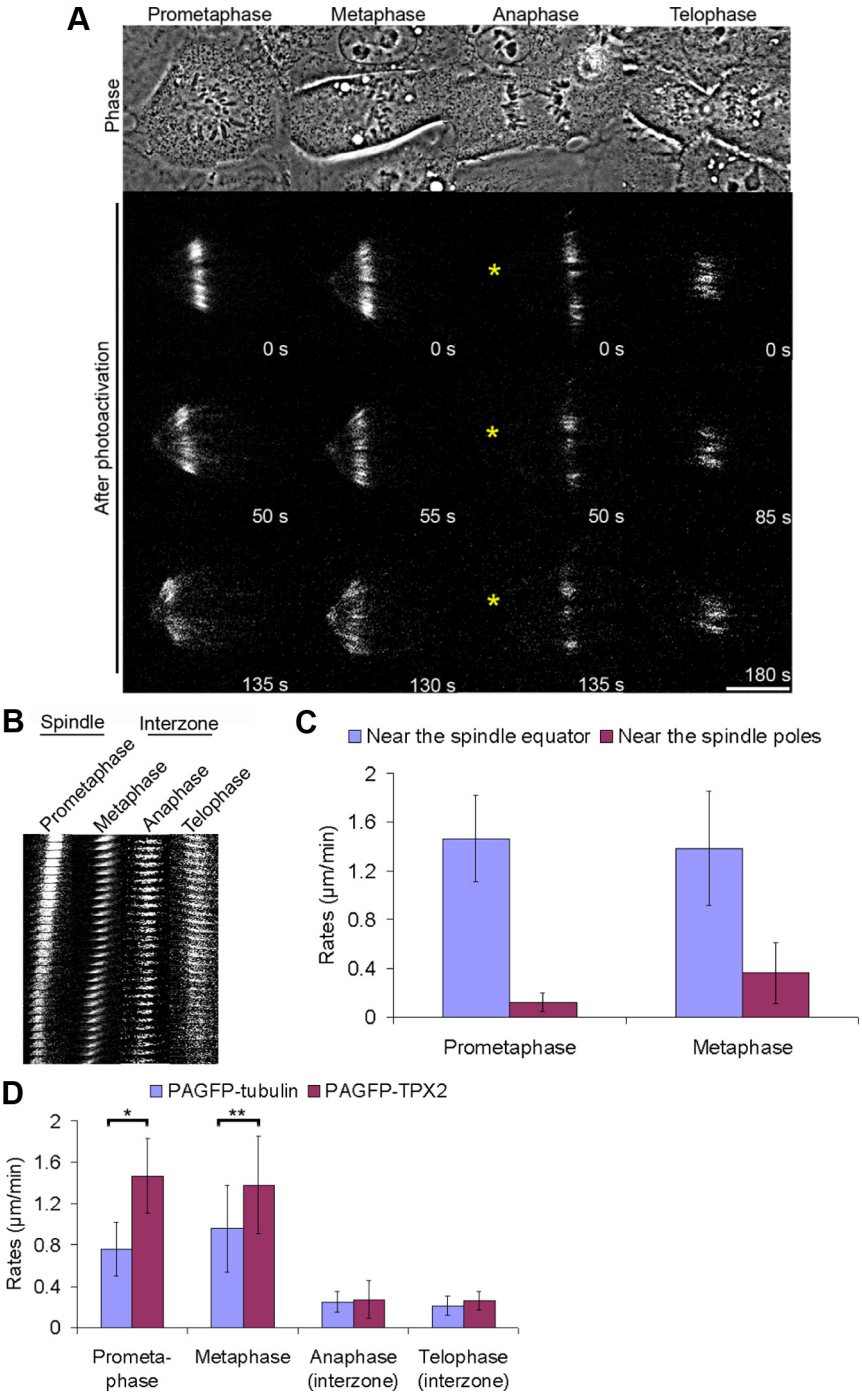

Figure 1. Movement of PA-GFP-TPX2 in the mitotic spindle. (A) Photoactivation of PA-GFP-TPX2 in LLC-Pk1 cells. Top row, phase contrast images of each cell before photoactivation; bottom rows, fluorescence images of PA-GFP-TPX2 for each cell. Time after photoactivation is shown in bottom right. Asterisks in the anaphase cell show the constant position of the spindle pole. (B) Kymographs of photoactivated marks from the cells shown in A. (C) Average rates of poleward motion of TPX2 near the equator and pole. (D) Average rates of poleward motion of TPX2 and PA-GFP-tubulin. For PA-GFP-tubulin, 14, 15, 9, and 10 cells were used to analyze poleward motion during prometaphase, metaphase, anaphase, and telophase, respectively. *$p < 0.01$ and **$p < 0.05$. Bar, 10 μm.

er's recommended dilution. Cyanine (Cy)3-labeled (Jackson ImmunoResearch Laboratories, West Grove, PA) or fluorescein isothiocyanate-labeled (Sigma-Aldrich) secondary antibodies were used at the recommended dilution for 60 min at 37°C. Coverslips were mounted in Vectashield containing 4′,6-diamidino-2-phenylindole to visualize DNA (Vector Laboratories, Burlingame, CA) and sealed with nail polish.

To measure the interkinetochore distance, LLC-Pk1 cells expressing green fluorescent protein (GFP)-CenpA were used. For nocodazole treatment, cells were incubated with 3.3 μM nocodazole for 4 h. Cells were transfected with mCherry TPX2 or mCherry TPX2-710 and examined at 48 h after transfection. The number of cells/kinetochore pairs analyzed were as follows: nocodazole-treated cells, 6/45; no transfection, nonaligned, 8/40; no transfection, aligned, 5/43; transfection with mCherry TPX2, aligned, 7/40; transfection with mCherry TPX2-710, aligned, 9/40; and transfection with mCherry TPX2, nonaligned, 6/42. For the experiments with transfected cells, we chose cells that contained similar levels of red fluorescence from the transfected protein.

Constructs, Protein Purification, and Small Interfering RNA (siRNA)

Photoactivatable (PA)-EGFP and mCherry-tagged TPX2 were generated by subcloning hTPX2 into pCMV-PA-EGFP or pCMV-mCherry (Trieselmann *et al*., 2003; Tulu *et al*., 2003). Nucleofection was performed using an Amaxa nucleofector following the protocol recommended by the manufacturer (Lonza Walkersville, Walkersville, MD). Cell lines expressing EGFP- or PA-EGFP-TPX2 were prepared as described previously (Wadsworth *et al*., 2005). Full-length human Eg5, the kind gift from Dr. Ann Blangley, was tagged with EGFP for transfection into mammalian cells. Proteins tagged with EGFP are referred to as having a GFP tag in this manuscript. The CC1 fragment of p150 was prepared as described previously (Ferenz and Wadsworth, 2007).

For glutathione transferase (GST) pull-down experiments, the N-terminal half of TPX2 (TNT, 1-364), the C-terminal half of TPX2 (TCT, 365-745), and TCT lacking the C-terminal 35 amino acids (TCTΔ35) were subcloned into pGEX-4T-1 (GE Healthcare, Little Chalfont, Buckinghamshire, United Kingdom) and purified from bacteria (BL-21). His-tagged Eg5 (amino acids 1-685, corresponding to the head-stalk region) was expressed in bacteria. GST pull-down was performed as described previously (Ma *et al*., 2009). In the experiment shown in Figure 4, 1/70 and one half the volume of supernatants and pellets were applied to the gel, respectively.

Image Acquisition, Photoactivation, and Inhibitors

Images were acquired using an Eclipse TE300 microscope (Nikon, Tokyo, Japan) equipped with a 100× phase numerical aperture 1.4 objective lens, a spinning disk confocal scan head (PerkinElmer, Wellesley, MA), and an Orca ER cooled charge-coupled device camera (Hamamatsu, Bridgewater, NJ). All images were taken using a dual-wavelength filter cube. Image acquisition was controlled by MetaMorph software (Molecular Devices, Sunnyvale, CA). Photoactivation was performed as described previously (Tulu *et al*., 2003; Ferenz and Wadsworth, 2007). Photoactivations that were performed within 3.5 μm of a spindle pole were defined as near the pole; photoactivation >3.5 μm from the nearest pole were defined as far from the pole.

The movement of photoactivated regions was measured as described, with the following modification. The position of the edge of the activated region closest to the chromosomes was tracked; in previous work, measurements were made using the edge of the activated region closest to the pole. Individual photoactivated regions, corresponding to bundles of kinetochore microtubules were used for these and our previous measurements. The values reported here differ from those reported previously because the poleward edge of the photoactivated mark moves faster than the edge nearest to the chromosomes (Ferenz and Wadsworth, 2007). In prometaphase and metaphase cells, spindle length remained constant as judged by spindle pole position, which was visible due to dim fluorescence of activated tubulin. Similarly, in anaphase cells, which were photoactivated in the interzonal region, pole-to-pole distance did not change over the time frame of the experiment (typically <3 min). In telophase cells, anaphase B was completed before photoactivation; spindle pole position was not marked in these cells due to the difficulty in precisely locating the spindle pole.

To inhibit microtubule dynamics, cells were incubated with nocodazole at 10 nM for 1 h before imaging. Antibodies to MCAK and Kif2a were used as described previously (Ferenz and Wadsworth, 2007). To inhibit dynein, cells were microinjected with p150 CC1 as described previously (Wadsworth, 1999). Before microinjection, all solutions were centrifuged at maximal speed in a microcentrifuge at 4°C through a syringe tip filter held in a microcentrifuge tube. siRNA to Eg5 was performed as described previously (Tulu *et al*., 2006) by using the sequence 5′-CUGAAGACCUGAAGACAAU-3′. Monastrol was prepared in dimethyl sulfoxide and used at 200 μM. To assay microtubule assembly near chromosomes and centrosomes, cells were incubated with 3.3 μM nocodazole for ~3 h before washout with drug-free medium (Tulu *et al*., 2006).

RESULTS

Characterization of LLC-Pk1 Cells Expressing EGFP- or PA-EGFP-TPX2

To examine the dynamic behavior of TPX2 in live cells, we transfected LLC-Pk1 cells with EGFP- or PA-EGFP–tagged TPX2 and generated cell lines expressing each fusion protein (Wadsworth *et al*., 2005; hereafter LLC-Pk1-GFP-TPX2 and LLC-Pk1-PA-GFP-TPX2). The distribution of the tagged proteins in live cells was indistinguishable from endogenous TPX2 observed in cells fixed and stained with antibodies to TPX2 (Supplemental Figure 1). Time-lapse imaging showed that GFP-TPX2 is nuclear during interphase (Wittmann *et al*., 2000; Gruss *et al*., 2002) and associates with microtubules immediately upon nuclear envelope breakdown. In prometaphase and metaphase cells, TPX2 localizes along spindle microtubules, but not detectably on polar astral microtubules, and is enriched toward the spindle poles. In anaphase and telophase cells, TPX2 localizes to interzonal and midbody microtubules, respectively (Supplemental Figure 1 and Supplemental Movie 1). Because overexpression of TPX2 has been reported previously to result in mitotic cells with aberrant spindle morphology (Garrett *et al*., 2002; Gruss *et al*., 2002), we quantified spindle morphology in both cell lines (Supplemental Figure 1). We found that the percentage of multipolar and monopolar spindles was increased in cells expressing either PA-GFP- or GFP-TPX2 as compared with parental cells. The mitotic index of GFP-TPX2 cells, but not PA-GFP-TPX2 cells, was reduced when compared with control cells. These features were not completely unexpected because the cells express both endogenous TPX2 and the

Table 1. Average rates of TPX2 transport

	Prometaphase		Metaphase		Anaphase (interzone)	Telophase (interzone)
	Near equator	Near pole	Near equator	Near pole		
Control	1.47 ± 0.38 (n = 19)	0.12 ± 0.08 (n = 12)	1.38 ± 0.47 (n = 16)	0.36 ± 0.25 (n = 11)	0.27 ± 0.18 (n = 11)	0.26 ± 0.09 (n = 10)
Nocodazole	0.71 ± 0.44 (n = 11)		0.81 ± 0.52 (n = 10)			
Kif2a/MCAK	0.66 ± 0.08 (n = 9)		0.91 ± 0.18 (n = 8)			
CC1	0.56 ± 0.41 (n = 11)		0.67 ± 0.53 (n = 12)			
Monastrol	0.48 ± 0.33 (n = 8)					
Eg5 RNAi	0.81 ± 0.53 (n = 13)					
CC1 + monastrol	0.31 ± 0.13 (n = 7)					

Data are averages ± SD. Values of TPX2 transport near spindle equator in any one column are significantly different from that column's control value ($p < 0.01$).

fluorescent construct. In addition, the fluorescent tag, which is located at the N terminus of TPX2, could interfere with the activation of Aurora A kinase (Bayliss *et al.*, 2003). The alternative strategy, placing the tag on the C terminus, was not used because the C terminus also mediates important aspects of TPX2 function (see below). However, only cells with morphologically normal mitotic spindles were selected for experiments, and these cells progressed through mitosis without any detectable abnormalities.

Region Specific Dynamics of TPX2 in Mitotic Cells

We measured the dynamic behavior of TPX2 and microtubules in LLC-Pk1 cells by using photoactivation of fluorescence (see *Materials and Methods*). TPX2 was photoactivated in the half-spindle of prometaphase and metaphase cells and on interzonal microtubules in anaphase and telophase cells (Figure 1A and Supplemental Movie 2). The average velocity of photoactivated marks was determined from kymographs (Ferenz and Wadsworth, 2007), by using the edge of the mark closest to the chromosomes (see *Materials and Methods*).

The results of these experiments demonstrate that TPX2 moves poleward in the half-spindle, at a rate of ~1.4 μm/min in metaphase and prometaphase cells (Table 1). In contrast, TPX2 on interzonal microtubules was nearly static (~0.3 μm/min) (Figure 1, A–C, and Table 1). Because motion of TPX2 in the half-spindle seemed to decrease near the pole (Figure 1B), we compared TPX2 transport after photoactivation near and far from the pole (see *Materials and Methods*). The data show that the rate of TPX2 motion was significantly decreased near spindle poles (Figure 1C and Table 1). Together, these results demonstrate that the dynamic behavior of TPX2 is regionally regulated in the mammalian mitotic spindle.

We also measured the rate of microtubule flux using photoactivation of PA-GFP-tubulin (Tulu *et al.*, 2003; Ferenz and Wadsworth, 2007). In the half-spindle of prometaphase and metaphase cells, microtubule flux occurs at average rates of 0.86 ± 0.3 and 0.96 ± 0.4 μm/min, respectively. These values are lower than reported previously for these cells because we measured the edge of the photoactivated mark near the chromosomes (see *Materials and Methods*). These values are consistent with rates of flux measured in other tissue culture cells (Cameron *et al.*, 2006). The rate of microtubule flux is statistically significantly different from the rate of TPX2 motion (Figure 1D). However, on interzonal microtubules in anaphase and telophase cells, the rate of motion of microtubules and TPX2 were not significantly different (Figure 1D). These results show that the poleward motion of TPX2 in metaphase cells occurs at a rate that is faster than microtubule flux in these cells.

Microtubule Flux Contributes to Poleward Motion of TPX2

Because TPX2 is a microtubule-binding protein (Schatz *et al.*, 2003), poleward flux of microtubules could contribute to motion of TPX2. We treated cells with low concentrations of nocodazole to suppress microtubule dynamics (Vasquez *et al.*, 1996) and reduce microtubule flux. Under these conditions, the rate of TPX2 poleward motion was significantly reduced in prometaphase and metaphase cells (Figure 2, A and B). To determine whether the slow motion of TPX2 in nocodazole-treated cells resulted from the slow, residual flux in these cells, we compared the rates of microtubule flux and TPX2 motion in nocodazole-treated cells (Figure 2C). The data show that the rate of microtubule flux is reduced to a greater extent than TPX2 motion, demonstrating that flux alone is not responsible for TPX2 motion under these conditions.

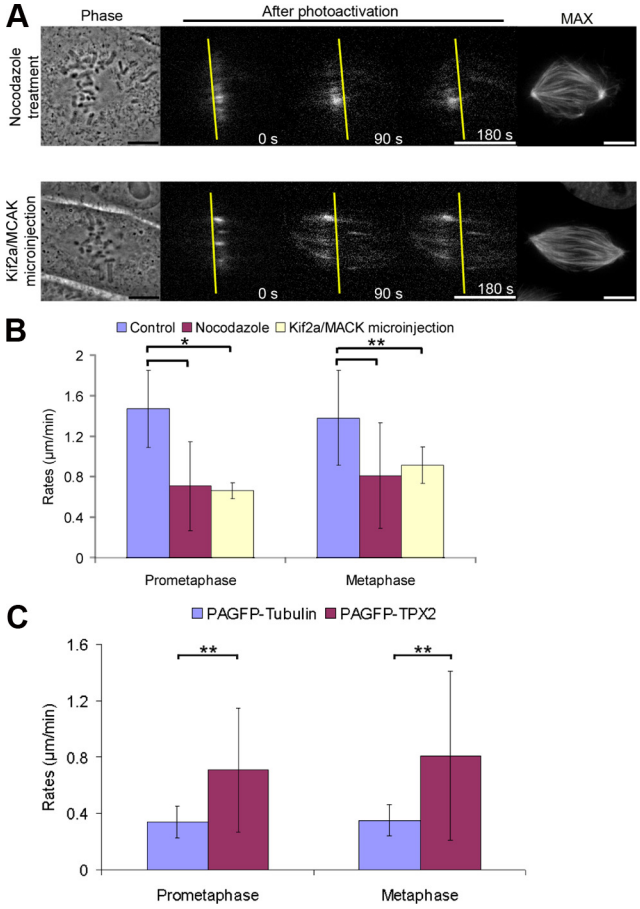

Figure 2. Poleward motion of TPX2 is sensitive to inhibition of microtubule flux. (A) Images of PA-GFP-TPX2-LLC-Pk1 cells treated with 10 nM nocodazole (top) or microinjected with anti-Kif2a and MCAK antibodies (bottom) and photoactivated. Left image is phase contrast, center images show selected images after photoactivation, and far right image shows maximal intensity projection after activation of the entire field of view. Yellow line is at a fixed position. (B) Average rates of poleward motion of TPX2 for control, nocodazole treated and anti-Kif2a/MCAK injected cells. Bars, 10 μm. *$p < 0.01$ and **$p < 0.05$. (C) Average rates of microtubule poleward motion (cells expressing PA-GFP-tubulin; n = 11) and TPX2 motion (cells expressing PA-GFP-TPX2; n = 11) in cells treated with low nocodazole. **$p < 0.05$.

In addition to reducing microtubule flux with nocodazole, we microinjected cells with antibodies directed against human Kif2a, a kinesin-13 that has been shown to be required for poleward flux of microtubules in human cells (Ganem *et al.*, 2005) and contribute to flux in LLC-Pk1 cells (Ferenz and Wadsworth, 2007). In this experiment, we also coinjected anti-MCAK antibodies, a treatment that prevents monopolar spindle formation after inhibition of Kif2a (Ganem *et al.*, 2005; Ferenz and Wadsworth, 2007). After microinjection, the rate of TPX2 poleward motion was reduced in both prometaphase and metaphase cells (Figure 2, A and B), further demonstrating that poleward motion of TPX2 in the half-spindle is sensitive to inhibition of microtubule flux.

The Distribution and Poleward Motion of TPX2 Are Sensitive to Inhibition of Dynein/Dynactin

TPX2 was originally identified as a factor that was required for the dynein-dependent localization of the kinesin Xklp2 to

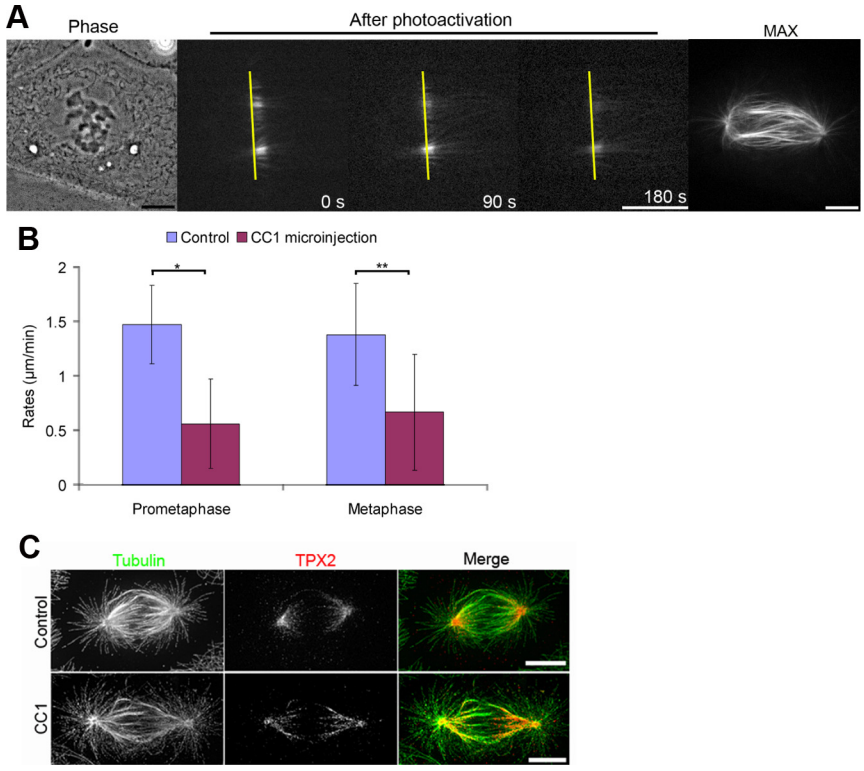

Figure 3. Poleward motion of TPX2 is sensitive to inhibition of dynein. (A) Images of PA-GFP-TPX2-LLC-Pk1 cells microinjected with CC1 before photoactivation. Left image is phase contrast, center images show selected images after photoactivation, and far right image shows maximal intensity projection after activation of the entire field of view. Yellow line is at a fixed position. (B) Average rates of poleward motion of TPX2 in control and CC1-injected prometaphase and metaphase cells. *$p < 0.01$ and **$p < 0.05$. (C) Distribution of TPX2 and microtubules in uninjected (top) and CC1-injected (bottom) cells. Bars, 10 μm.

spindle poles (Wittmann *et al*., 2000), suggesting that dynein is required for TPX2 transport. To examine this possibility, cells were microinjected with the CC1 fragment of the p150 subunit of dynactin, a treatment that interferes with the dynein–dynactin interaction and blocks dynein-dependent processes in cells (Quintyne *et al*., 1999; Gaetz and Kapoor, 2004; Ferenz and Wadsworth, 2007). The results show that the rate of poleward motion of TPX2 in prometaphase and metaphase cells is reduced after microinjection of CC1 (Figure 3, A and B, and Supplemental Movie 3). Furthermore, TPX2 was more uniformly distributed along spindle fibers in CC1 injected compared with control cells (Figure 3C). Inhibition of dynein/dynactin by microinjection of CC1 resulted in accumulation of the p150 subunit of dynactin at kinetochores but did not alter the localization of Kif2a at spindle poles (Supplemental Figure 2, A and B), consistent with previous work (Howell *et al*., 2001; Ferenz and Wadsworth, 2007).

Poleward Motion of TPX2 Requires an Interaction with Eg5

A direct interaction between the C-terminal 35 amino acids of TPX2 and Eg5 has been demonstrated using purified *X. laevis* proteins (Eckerdt *et al*., 2008), and each protein has been reported to accumulate at spindle poles. We examined the distribution of myc-GFP-Eg5 and mCherry-TPX2 in LLC-Pk1 cells throughout mitosis by using spinning disk confocal microscopy. We found that the two proteins colocalized along spindle microtubules from prophase to anaphase and were enriched at spindle poles. In telophase cells, TPX2, but not Eg5, associated with bundles of midbody microtubules (Supplemental Figure 1E).

Next, we examined the contribution of Eg5 to poleward motion of TPX2 in the mammalian spindle. Because poleward transport of TPX2 and Eg5 in the half-spindle are dynein dependent (Uteng *et al*., 2008), we hypothesized that Eg5 could contribute to transport by linking TPX2 to dynein. To test this, we measured poleward motion of TPX2 in cells that were treated with siRNA to deplete, or monastrol to inhibit, Eg5 (Mayer *et al*., 1999). Poleward movement of TPX2 was dramatically reduced on monastrol-induced monopolar spindles, compared with motion in untreated prometaphase cells (Figure 4, A and C). In Eg5 siRNA-treated cells, poleward movement of TPX2 was also statistically significantly reduced, compared with untreated prometaphase cells (Figure 4, A and C, and Supplemental Movie 4). Poleward motion of TPX2 in monastrol-treated and siRNA-depleted cells was not significantly different ($p = 0.23$).

To determine whether mammalian TPX2 and Eg5 interact, we performed GST pull-down assays using the C- or N-terminal half of TPX2 (TCT and TNT), or TCT lacking the last 35 amino acids (TCTΔ35), each tagged with GST and a human Eg5 head-stalk construct (Eg5HS) (Trieselmann *et al*., 2003; Eckerdt *et al*., 2008). The results showed that Eg5HS interacted with the TCT fragment more strongly than with TNT or TCTΔ35 (Figure 4B). This interaction is likely to be weak or dynamic, because only a fraction of the input protein was recovered. Consistent with this possibility, standard immunoprecipitation failed to show an interaction between Eg5 and TPX2 (data not shown).

To determine whether the C terminus of TPX2 is important for poleward motion, we tagged TPX2 lacking the terminal 35 amino acids (TPX2-710) with PA-GFP and performed photoactivation. For this experiment, we selected cells containing morphologically normal bipolar spindles (see below). After photoactivation in the half-spindle, poleward motion of PA-GFP-TPX2-710 was greatly reduced, compared with control cells, and the photoactivated protein rapidly redistributed throughout the spindle (Figure 4D and Supplemental Movie 5). These data show that TPX2 and Eg5 colocalize in mammalian cells, that the purified mammalian

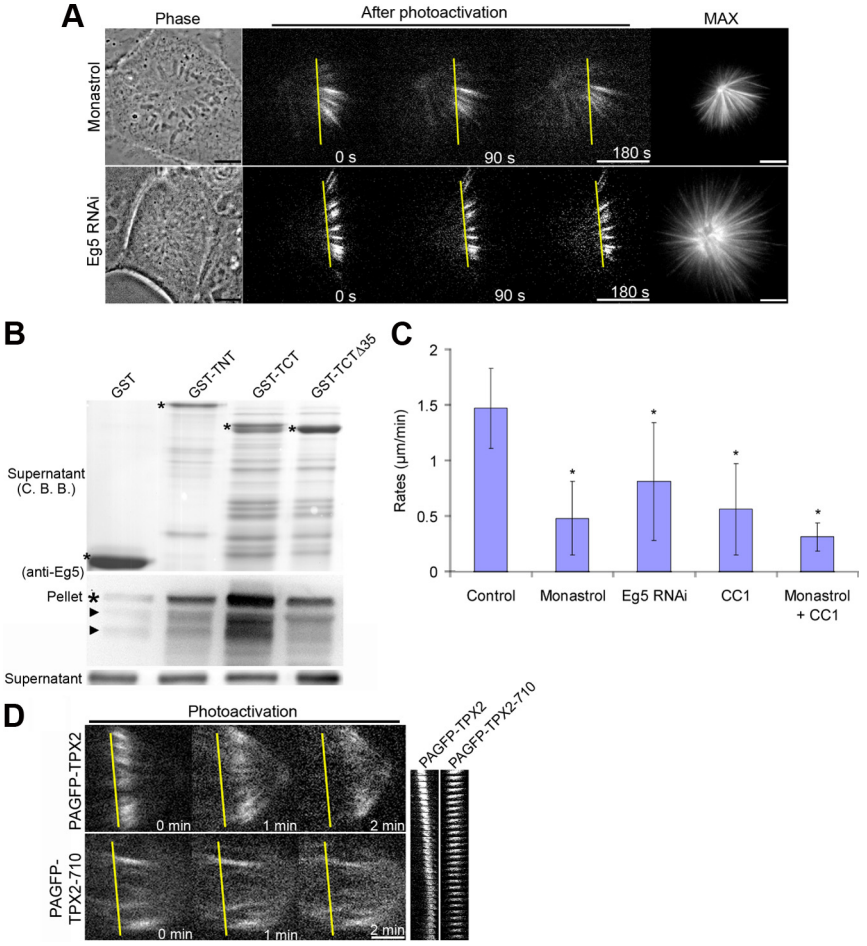

Figure 4. Poleward motion of TPX2 requires an interaction with Eg5. (A) Images of PA-GFP-TPX2-LLC-Pk1 cells treated with monastrol (top) or with siRNA targeting Eg5 before photoactivation. Left image is phase contrast, center images show selected images after photoactivation, and far right image shows maximal intensity projection after activation of the entire field of view. Yellow line is at a fixed position. (B) GST pull-down. Top, Coomassie Blue-stained gel (CBB); asterisks mark the major bands of protein in each lane. Bottom, Western blot probed with Eg5 antibodies; the supernatant and pelleted fractions of the pull-down are shown. (C) Average rates of motion for cells treated with the indicated inhibitors. *$p < 0.01$. (D) Photoactivation of PA-GFP-TPX2 (top) and PA-GFP-TPX2-710 (bottom); kymographs are on the right. Note that in the cell expressing PA-GFP-TPX2-710 fluorescence is distributed along the length of the microtubules within 1 min of photoactivation. Bars, 10 μm.

proteins interact in vitro and that the C terminus of TPX2 is required for efficient poleward transport.

TPX2/Eg5 Interaction Regulates the Organization and Stability of Kinetochore Microtubules

To determine whether the TPX2–Eg5 interaction contributes to microtubule organization during spindle formation, we examined live and fixed cells overexpressing mCherry-tagged full-length TPX2 or TPX2-710. Both full-length TPX2 and TPX2-710 associated with microtubules in transfected cells (Figure 5, A and C, and Supplemental Figure 3). In live cells expressing GFP-tubulin, expression of TPX2-710 resulted in a disorganized spindle, characterized by bundles of microtubules near chromosomes, and failure to progress through mitosis (Figure 5A and Supplemental Movie 6). We quantified the spindle phenotype using fixed cells (Figure 5, B and C). Approximately 40% of cells expressing TPX2-710 showed a disorganized spindle, characterized by microtubules extending into the cell periphery and bundles of microtubules near chromosomes, and defects in chromosome alignment. The remainder of the cells had normal bipolar or collapsed monopolar spindles. Mitotic spindles in cells overexpressing full-length TPX2 were either bipoles or monopoles, consistent with previous work showing that overexpression of TPX2 induces spindle shortening (Figure 5, A and C, and Supplemental Figure 3; Eckerdt *et al.*, 2008). Less than 10% of cells expressing full-length TPX2 showed a disorganized spindle phenotype. These results show that expression of TPX2-710 results in supernumerary microtubules in the cell periphery and disorganized bundles of microtubules near chromosomes.

To determine whether the microtubule bundles formed near chromosomes corresponded to kinetochore fibers, we fixed and stained cells expressing TPX2-710 to visualize microtubules and kinetochores (Figure 5C). In control cells, and cells expressing full-length TPX2, bundles of microtubules terminated at Hec1-positive kinetochores (Figure 5C, top and middle, insets). In cells expressing TPX2-710, some of the microtubule bundles that form in these cells terminate at Hec1-positive sites, but unattached kinetochores and syntelic attachments, were frequently observed (Figure 5C, bottom, insets).

Next, we examined microtubule stability in TPX2-transfected cells. Bundles of microtubules in cells expressing TPX2 or TPX2-710 were present after incubation at 4°C for 20 min (Yang *et al.*, 2007), a treatment that disassembles labile microtubules but not kinetochore fiber microtubules. However, unlike microtubule bundles in control cells or cells expressing full-length TPX2, microtubule bundles in cells expressing TPX2-710 were disorganized (Figure 5D).

Finally, because many chromosomes failed to align at the spindle equator in the cells overexpressing TPX2-710, we measured the interkinetochore distance in control cells and cells expressing TPX2 or TPX2-710 (Figure 5E). The results show that interkinetochore distance was statistically significantly decreased in cells expressing truncated TPX2 compared with control metaphase cells and with cells expressing full-length TPX2. Interkinetochore distance was also re-

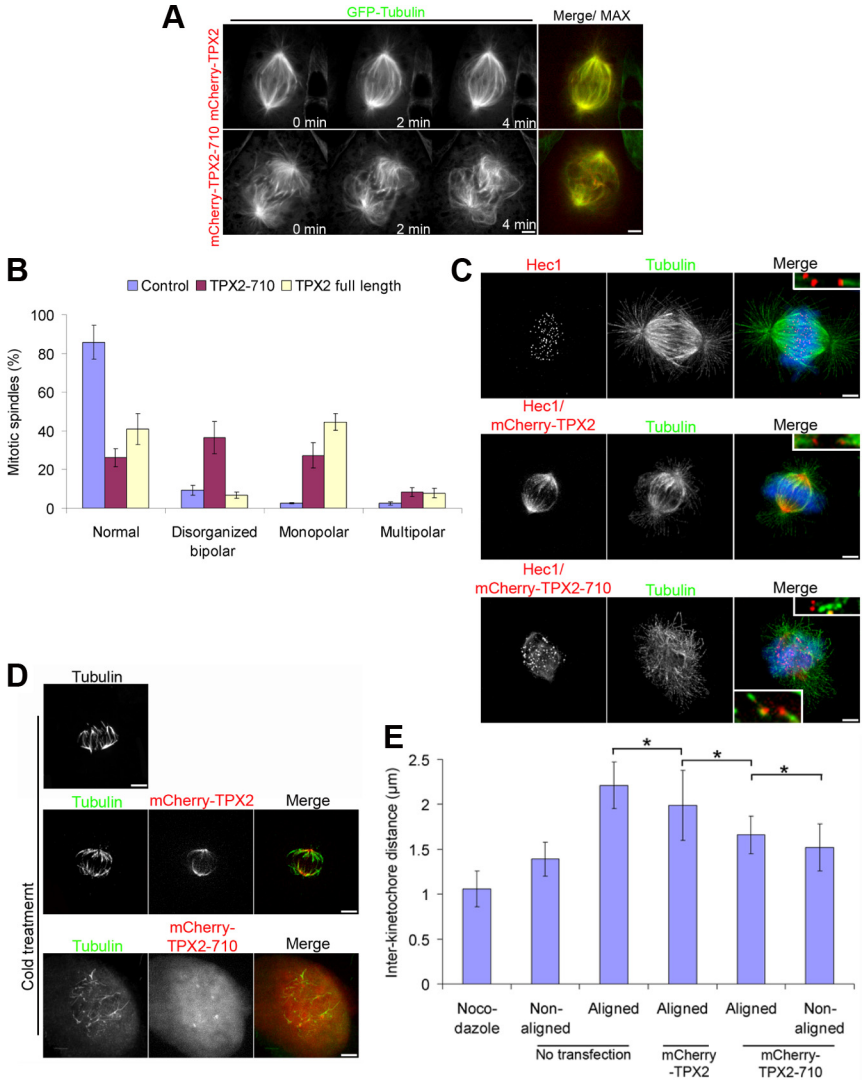

Figure 5. Organization of kinetochore fiber microtubules requires the C terminus of TPX2. (A) LLC-Pk1-α cells expressing full-length (top) or mCherryTPX2–710 (bottom); merged images on the right. (B) Quantification of spindle phenotypes. Values represent the mean of three independent experiments ± SD; at least 100 cells were counted for each experiment. (C) Spindle morphology in control, untransfected cells (top), and cells transfected with full-length (middle), or TPX2-710 (bottom). Panels show DNA, Hec1/mCherryTPX2, microtubules, and merged. Insets show higher magnification of microtubule bundles and Hec1 staining. (D) Microtubules in control (top) and cells transfected withTPX2 (middle) or TPX2-710 after treatment at 4°C. (E) Interkinetochore tension in nocodazole treated cells, nonaligned and aligned chromosomes in control untransfected cells, aligned chromosomes in cells expressing full-length mCherryTPX2, and aligned and nonaligned chromosomes in cells expressing TPX2-710. *$p < 0.01$.

duced in cells expressing full-length TPX2 compared with control cells. These results demonstrate that expression of truncated TPX2 interferes with chromosome alignment and development of interkinetochore tension.

To determine whether the TPX2–Eg5 interaction impacts microtubule formation near chromosomes, we used a nocodazole washout assay (Tulu *et al.*, 2006). When control LLC-Pk1 cells expressing GFP-tubulin are released from nocodazole, microtubules assemble near chromosomes and at centrosomes and subsequently coalesce to form a bipolar spindle (Figure 6A and Supplemental Movie 7). In contrast, when cells expressing full-length or TPX2-710 were released from nocodazole, microtubule formation in the chromosome region was greatly enhanced and coalescence of microtubule foci into a bipolar spindle failed (Figure 6A and Supplemental Movies 8 and 9). In some cases, discrete puncta of fluorescence were observed in the chromosome region, probably corresponding to microtubules forming at kinetochores (Figure 6A, bottom, 36 min). Because the level of overexpression of each protein varies in the transfected cells, we could not quantitatively compare the extent of microtubule formation in these experiments. However, although both full-length and truncated TPX2 promoted microtubule formation near chromosomes in this assay, only full-length TPX2 accumulated at the center of microtubule foci, whereas the truncated protein was mostly diffuse (Figure 6A, right), consistent with its behavior after photoactivation.

DISCUSSION

The results of our experiments demonstrate that TPX2 in the half-spindle is transported toward spindle poles during prometaphase and metaphase of mitosis. TPX2 in the interzone, and near spindle poles, is transported much more slowly. Poleward transport of TPX2 is sensitive to inhibition of dynein, Eg5, and microtubule flux. Transport requires the C-terminal 35 amino acids of TPX2, and overexpression of TPX2 lacking this domain results in defects in kinetochore fiber formation, chromosome attachment, spindle formation and mitotic progression. Our results demonstrate that the dynamics of TPX2 in the spindle is regionally regulated and that an interaction of TPX2 with Eg5 is important for spindle microtubule organization and kinetochore fiber formation.

Regional Regulation of TPX2 Transport

It is well established that spindle microtubules move poleward in mitotic cells, but our understanding of the dynamic behavior of other spindle components is still incomplete.

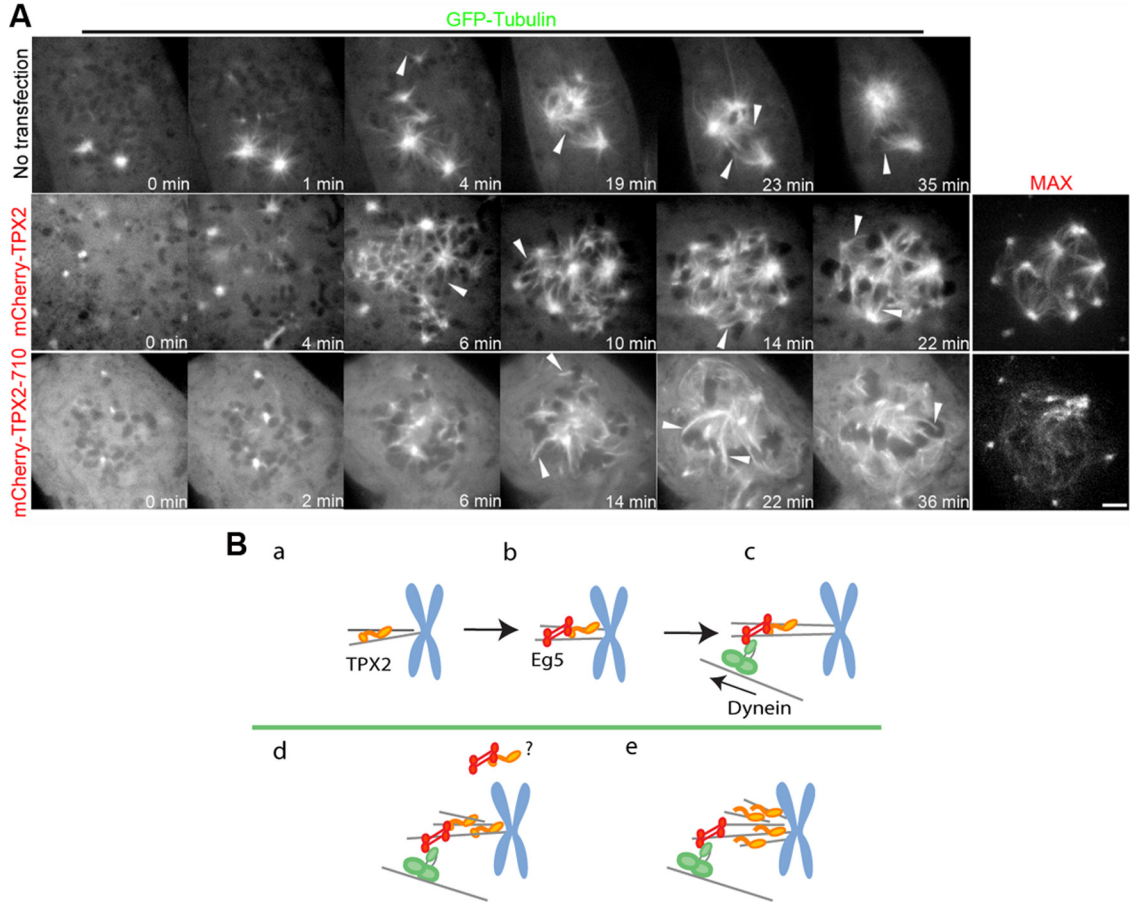

Figure 6. Microtubule bundle formation near chromatin in cells expressing TPX2 and TPX2-710. (A) Microtubule formation after release from nocodazole in live cells expressing GFP-tubulin. Selected frames from time-lapse sequences of control cells (top row) or cells transfected with full-length mCherry-TPX2 (middle row) or mCherry-TPX2-710 (bottom row). Time is in minutes:seconds after release from nocodazole. Arrowheads mark kinetochore-fiber-like bundles of microtubules. Bars, 10 μm. (B) Model for TPX2 behavior. Kinetochore fiber formation in control cells (a–c)and in cells overexpressing full-length TPX2 (d) or TPX2-710 (e).

Recent work shows that the mitotic motor Eg5 is transported toward microtubule minus ends in the half-spindle of *Xenopus* extract spindles in a dynein-dependent manner and is static in the interzone (Uteng *et al.*, 2008). In *Drosophila* cells, Eg5 rapidly exchanges with spindle microtubules, making short poleward excursions (Cheerambathur *et al.*, 2008). We now show that TPX2, like Eg5 in *X. laevis* spindles, is transported poleward in the half-spindle and is static on interzonal microtubules and near spindle poles (Uteng *et al.*, 2008). In LLC-Pk1 cells during anaphase and telophase, spindle elongation overlaps temporally with chromosome-to-pole motion and was typically completed before photoactivation of interzonal microtubules. Thus, the absence of poleward motion of TPX2 in the interzone could result because TPX2 is bound to static, or slowly moving, microtubules and/or static Eg5 in the interzone (Uteng *et al.*, 2008).

Our data support the view that motion of TPX2 in the half-spindle results from transport along fluxing microtubules. First, TPX2 motion was faster than microtubule flux in these cells, suggesting that flux alone cannot account for the poleward motion of TPX2. Second, in cells treated to reduce microtubule flux, the motion of TPX2 was faster than the residual microtubule flux. Third, the extent to which TPX2 motion in the half-spindle was reduced after inhibition of dynein or Eg5 was greater than the extent to which these same inhibitors altered microtubule flux (Ferenz and Wadsworth, 2007). Finally, the observation that TPX2-710 fails to move poleward but shows diffuse labeling along microtubules after photoactivation, supports the idea that TPX2 motion is dependent on an interaction with Eg5.

Dynein-dependent Poleward Transport

Many spindle components are enriched at spindle poles, and in several cases dynein contributes to this accumulation. For example, the microtubule-associated protein NuMA directly interacts with dynein/dynactin for transport to spindle poles, where it contributes to pole focusing (Merdes *et al.*, 2000). Poleward motion of spindle assembly checkpoint proteins is also dynein dependent, but how dynein/dynactin mediates this transport is not yet clear (Howell *et al.*, 2001). Numerous other proteins accumulate at spindle poles, but the contribution, if any, of dynein has not been determined (i.e., XMAP215). Here, we show that TPX2 moves poleward in a dynein-dependent manner and that this is mediated by an interaction with Eg5.

Understanding how dynein mediates transport of spindle components is complicated by the fact that dynein also contributes to spindle microtubule organization and motion (Gaglio *et al.*, 1997; Heald *et al.*, 1997; Ferenz and Wadsworth, 2007). Although poleward microtubule motion, or flux, has been reported to be insensitive to inhibition of dynein (Sawin and Mitchison, 1991; Maiato *et al.*, 2005; Cameron *et al.*,

2006; Ferenz and Wadsworth, 2007), recent studies show that spindle flux has two velocity modes and that the flux rate is reduced near spindle poles (Yang *et al*., 2008). Inhibition of dynein activity shifts the velocity distribution to a single mode and eliminates the regional variation in flux rate, demonstrating that dynein contributes to spindle microtubule flux behavior (Yang *et al*., 2008). We observed that, like microtubule flux, TPX2 transport is greatly reduced near spindle poles. Regional differences in TPX2 behavior could result from differences in microtubule behavior near and far from the spindle pole, association of TPX2 with distinct classes of spindle microtubules, differences in motor behavior in different spindle locations, and/or distance from the chromosome derived Ran-gradient (Kalab *et al*., 2006). Understanding the regulation of spindle microtubule organization and transport is an important goal of future studies.

What Might Be the Role of Poleward Transport of TPX2?

TPX2 is required for microtubule assembly in the chromatin-dependent spindle assembly pathway and the N-terminal Aurora A interacting domain of TPX2 is essential for this activity (Bird and Hyman, 2008). Cells expressing TPX2 lacking the Aurora A interacting region, or with point mutations that block the TPX2-Aurora A interaction, assemble functional bipolar spindles that are very short (Bird and Hyman, 2008). The C-terminal half of TPX2 is required for its spindle localization and overexpression of a large C-terminal domain blocks centrosome separation in cultured *Xenopus* cells (Brunet *et al*., 2004; Eckerdt *et al*., 2008). Microinjection of excess Eg5 rescues this defect, demonstrating that an interaction with TPX2 regulates Eg5 function in vivo (Eckerdt *et al*., 2008). In addition to these activities, we show that overexpression of TPX2-710, but not full-length TPX2, results in the formation of extensive bundles of microtubules near chromosomes in intact cells. Based on this observation, we hypothesize that poleward transport of TPX2 down regulates the microtubule-nucleating activity of TPX2 near kinetochores. In the nocodazole washout assay, both full-length TPX2 and TPX2-710 induced extensive microtubule formation near chromosomes, further emphasizing the need for regulation of TPX2 activity during spindle formation.

Our observations are consistent with a model (Figure 6B) in which Ran in the vicinity of chromosomes activates TPX2 leading to microtubule formation (Figure 6Ba), either directly or by activation of other Ran-dependent proteins (Trieselmann *et al*., 2003; Groen *et al*., 2009). Chromosome-associated microtubules are then organized into mature kinetochore fibers and incorporated into the spindle in an Eg5 and dynein-dependent manner (Figure 6B, b and c) (Maiato *et al*., 2004). Expression of full-length TPX2 can induce spindle shortening, a phenotype that may result from inhibition of Eg5-generated outward forces (Eckerdt *et al*., 2008) (Figure 6Bc, question mark in d) but does not detectably alter kinetochore fiber formation (Figure 6Bd). In contrast, interfering with the Eg5/TPX2 interaction, by expression of TPX2-710, results in excessive microtubule formation near chromosomes (Figure 6Be) and defects in chromosome alignment, kinetochore fiber organization, and mitotic progression. Our results demonstrate that the interaction between TPX2 and Eg5 is important for kinetochore fiber formation and may function to link microtubules formed in the chromosome-dependent pathway to dynein for incorporation into the spindle.

ACKNOWLEDGMENTS

We thank the members of the Lee and Ross laboratories (University of Massachusetts, Amherst, MA) for constructive comments during the course of this work and Dr. L. Collins for reading the manuscript. We thank Drs. Alexey Khodjakov (Wadsworth Center, New York State Department of Health, Albany, NY) and Claire Walczak (Indiana University, Bloomington, IN) for antibodies, Drs. George Patterson and Jennifer Lippincott-Schwartz (National Institutes of Health, Bethesda, MD) for PA-GFP, and Drs. Anne Blangy (Centre de Recherches de Biochimie and Macromoléculaire, Montpellier, France) and Susan Gilbert (Rennselaer Polytechnic Institute, Troy, NY) for Eg5 constructs. We especially thank Dr. John Willoughby (University of Massachusetts) for advice and reagents for the GST pull-down experiments. This work was supported by grant GM 59057 from the National Institutes of Health (to P. W.) and a Canadian Cancer Society grant (to A.W.).

REFERENCES

Bayliss, R., Sardon, T., Vernos, I., and Conti, E. (2003). Structural basis of Aurora A activation by TPX2 at the mitotic spindle. Mol. Cell. *12*, 851–862.

Bird, A. W., and Hyman, A. A. (2008). Building a spindle of the correct length in human cells requires the interaction between TPX2 and Aurora A. J. Cell Biol. *182*, 289–300.

Blangy, A., Arnaud, L., and Nigg, E. A. (1997). Phosphorylation by $p34^{cdc2}$ protein kinase regulates binding of the kinesin related motor HsEg5 to the dynactin subunit $p150^{glued}$. J. Biol. Chem. *272*, 19418–19424.

Brunet, S., Sardon, T., Zimmerman, T., Wittman, T., Pepperkok, R., Karsenti, E., and Vernos, I. (2004). Characterization of the TPX2 domains involved in microtubule nucleation and spindle assembly in *Xenopus* egg extracts. Mol. Biol. Cell. *15*, 5318–5328.

Burbank, K. S., Mitchison, T. J., and Fisher, D. S. (2007). Slide-and-cluster models for spindle assembly. Curr. Biol. *17*, 1373–1383.

Cameron, L. A., Yang, G., Cimini, D., Canman, J. C., Kisurina-Evgenieva, O., Khodjakov, A., Danuser, G., and Salmon, E. D. (2006). Kinesin 5-independent poleward flux of kinetochore microtubules in PtK1 cells. J. Cell Biol. *173*, 173–179.

Cheerambathur, D. K., Brust-Mascher, I., Civelekoglu-Scholey, G., and Scholey, J. M. (2008). Dynamic partitioning of mitotic kinesin-5 cross-linkers between microtubule-bound and freely diffusing states. J. Cell Biol. *182*, 429–436.

Eckerdt, F., Eyers, P. A., Lewellyn, A. L., Prigent, C., and Maller, J. L. (2008). Spindle pole regulation by a discrete Eg5-interacting domain in TPX2. Curr. Biol. *18*, 519–525.

Ferenz, N. P., and Wadsworth, P. (2007). Prophase microtubule arrays undergo flux-like behavior in mammalian cells. Mol. Biol. Cell. *18*, 3993–4002.

Gaetz, J., and Kapoor, T. M. (2004). Dynein/dynactin regulate metaphase spindle length by targeting depolymerizing activities to spindle poles. J. Cell Biol. *166*, 465–471.

Gaglio, T., Dionne, M. A., and Compton, D. A. (1997). Mitotic spindle poles are organized by structural and motor proteins in addition to centrosomes. J. Cell Biol. *138*, 1055–1066.

Ganem, N. J., Upton, K., and Compton, D. A. (2005). Efficient mitosis in human cells lacking polewards microtubule flux. Curr. Biol. *15*, 1827–1832.

Garrett, S., Auer, K., Compton, D. A., and Kapoor, T. (2002). hTPX2 is required for normal spindle morphology and centrosome integrity during vertebrate cell division. Curr. Biol. *12*, 2055–2059.

Groen, A. C., Maresca, T. J., Gatlin, J. C., Salmon, E. D., and Mitchison, T. J. (2009). Functional overlap of microtubule assembly factors in chromatin-promoted spindle assembly. Mol. Biol. Cell *20*, 2766–2773.

Gruss, O. J., Wittmann, M., Yokoyama, H., Pepperkok, R., Kufer, T., Sillje, H., Karsenti, E., Mattaj, I. W., and Vernos, I. (2002). Chromosome-induced microtubule assembly mediated by TPX2 is required for spindle formation in HeLa cells. Nat. Cell Biol. *4*, 871–879.

Heald, R., Tournebize, R., Blank, T., Sandaltzopoulos, R., Becker, P., Hyman, A., and Karsenti, E. (1996). Self-organization of microtubules into bipolar spindles around artificial chromosomes in *Xenopus* egg extracts. Nature *382*, 420–425.

Heald, R., Tournebize, R., Habermann, A., Karsenti, E., and Hyman, A. (1997). Spindle assembly in *Xenopus* egg extracts: respective roles of centrosomes and microtubule self-organization. J. Cell Biol. *138*, 615–628.

Hinchcliffe, E. H., Cham, M., Khodjakov, A., and Sluder, G. (2001). Requirement of a centrosomal activity for cell cycle progression through G1 into S phase. Science *291*, 1547–1550.

Howell, B. J., McEwen, B. F., Canman, J. C., Hoffman, D. B., Farrar, E. M., Rieder, C. L., and Salmon, E. D. (2001). Cytoplasmic dynein/dynactin drives kinetochore protein transport to the spindle poles and has a role in mitotic spindle checkpoint inactivation. J. Cell Biol. *155*, 1159–1172.

Kalab, P., Pralle, A., Isacoff, E. Y., and Weis, K. (2006). Analysis of a RanGTP-regulated gradient in mitotic somatic cells. Nature *440*, 697–701.

Khodjakov, A., Cole, R. W., Oakley, B. R., and Rieder, C. L. (2000). Centrosome-independent mitotic spindle formation in vertebrates. Curr. Biol. *10*, 59–67.

Khodjakov, A., Copenagle, L., Gordon, M. B., Compton, D. A., and Kapoor, T. (2003). Minus-end capture of preformed kinetochore fibers contributes to spindle morphogenesis. J. Cell Biol. *160*, 671–683.

Kirschner, M. W., and Mitchison, T. (1986). Beyond self-assembly: from microtubules to morphogenesis. Cell *45*, 329–342.

Koffa, M. D., Casanova, C. M., Santarella, R., Kocher, T., Wilm, M., and Mattaj, I. W. (2006). HURP is part of a ran-dependent complex involved in spindle formation. Curr. Biol. *16*, 743–754.

Ma, N., M.-Tsai, Y., Wang, S., Lu, B., Chen, R., Yates, J.R.I., Zhu, X., and Zheng, Y. (2009). Requirement for Nudel and dynein for assembly of the lamin B spindle matrix. Nat. Cell Biol. *11*, 247–256.

Maiato, H., Khodjakov, A., and Rieder, C. L. (2005). Drosophila CLASP is required for the incorporation of microtubule subunits into fluxing kinetochore fibres. Nat. Cell Biol. *7*, 42–47.

Maiato, H., Rieder, C. L., and Khodjakov, A. (2004). Kinetochore-driven formation of kinetochore fibers contributes to spindle assembly during animal mitosis. J. Cell Biol. *167*, 831–840.

Mayer, T. U., Kapoor, T. M., Haggarty, S. J., King, R. W., Schreiber, S. L., and Mitchison, T. J. (1999). Small molecule inhibitor of mitotic spindle bipolarity identified in a phenotype-based screen. Science *286*, 971–974.

Merdes, A., Heald, R., Samejima, K., Earnshaw, W. C., and Cleveland, D. W. (2000). Formation of spindle poles by dynein/dynactin-dependent transport of NuMA. J. Cell Biol. *149*, 851–861.

Mitchison, T. J. (1989). Polewards microtubule flux in the mitotic spindle: evidence from photoactivation of fluorescence. J. Cell Biol. *109*, 637–652.

Mitchison, T. J., and Kirschner, M. W. (1984). Dynamic instability of microtubule growth. Nature *312*, 237–242.

Quintyne, N. J., Gill, S. R., Eckley, D. M., Crego, C. L., Compton, D. A., and Schroer, T. A. (1999). Dynactin is required for microtubule anchoring at fibroblast centrosomes. J. Cell Biol. *147*, 321–334.

Rogers, G. C., Rogers, S. L., and Sharp, D. J. (2005). Spindle microtubules in flux. J. Cell Sci. *118*, 1105–1116.

Sawin, K. E., and Mitchison, T. J. (1991). Poleward microtubule flux in mitotic spindles assembled *in vitro*. J. Cell Biol. *112*, 941–954.

Schatz, C. A., Samntarella, R., Hoenger, A., Karsenti, E., Mattaj, I. W., Gruss, O. J., and Carazo-Salas, R. E. (2003). Importin a-regulated nucleation of microtubules by TPX2. EMBO J. *22*, 2060–2070.

Trieselmann, N., Armstrong, S., Rauw, J., and Wilde, A. (2003). Ran modulates spindle assembly by regulating a subset of TPX2 and Kid activities including Aurora A activation. J. Cell Sci. *116*, 4791–4798.

Tulu, U. S., Fagerstrom, C., Ferenz, N. P., and Wadsworth, P. (2006). Molecular requirements for kinetochore-associated microtubule formation in mammalian cells. Curr. Biol. *16*, 536–541.

Tulu, U. S., Rusan, N., and Wadsworth, P. (2003). Peripheral, non-centrosome-associated microtubules contribute to spindle formation in centrosome containing cells. Curr. Biol. *13*, 1894–1899.

Uteng, M., Hentrich, C., Bieling, P., and Surrey, T. (2008). Poleward transport of Eg5 by dynein-dynactin in *Xenopus* egg extract spindles. J. Cell Biol. *182*, 715–726.

Vasquez, R. J., Howell, B., Yvon, A. C., Wadsworth, P., and Cassimeris, L. (1996). Nanomolar concentrations of nocodazole alter microtubule dynamic instability *in vivo* and *in vitro*. Mol. Biol. Cell. *8*, 973–985.

Wadsworth, P. (1999). Microinjection of mitotic cells. Methods Cell Biol. *61*, 219–231.

Wadsworth, P., Rusan, N. M., Tulu, U. S., and Fagerstrom, C. (2005). Stable expression of fluorescently tagged proteins for studies of mitosis in mammalian cells. Nat. Methods *2*, 981–987.

Wilde, A., and Zheng, Y. (1999). Stimulation of microtubule aster formation and spindle assembly by the small GTPase Ran. Science *284*, 1359–1362.

Wittmann, T., Boleti, H., Antony, C., Karsenti, E., and Vernos, I. (1998). Localization of the kinesin-like protein Xklp2 to spindle poles requires a leucine zipper, a microtubule-associated protein and dynein. J. Cell Biol. *143*, 673–685.

Wittmann, T., Wilm, M., Karsenti, E., and Vernos, I. (2000). TPX2, a novel *Xenopus* MAP involved in spindle pole organization. J. Cell Biol. *149*, 1405–1418.

Yang, G., Cameron, L. A., Maddox, P. S., Salmon, E. D., and Danuser, G. (2008). Regional variation of microtubule flux reveals microtubule organization in the metaphase spindle. J. Cell Biol. *182*, 631–639.

Yang, Z., Tulu, U. S., Wadsworth, P., and Rieder, C. L. (2007). Kinetochore dynein is required for normal chromosome motion and congression independent of the spindle assembly checkpoint. Curr. Biol. *17*, 973–980.